

# Localization of solitons: linear response of the mean-field ground state to weak external potentials

C.A. Müller

Received: 26 July 2010 / Revised version: 28 September 2010 / Published online: 11 February 2011  
© Springer-Verlag 2011

**Abstract** Two aspects of bright matter-wave solitons in weak external potentials are discussed. First, we briefly review recent results on the Anderson localization of an entire soliton in disordered potentials, as a paradigmatic showcase of genuine quantum dynamics beyond simple perturbation theory. Second, we calculate the linear response of the mean-field soliton shape to a weak, but otherwise arbitrary, external potential, with a detailed application to lattice potentials.

## 1 Introduction

Recently, the cold-atom community has shown renewed interest in soliton dynamics, sparked by the experimental observation of cold-atom solitons in quasi-one-dimensional Bose–Einstein condensates with attractive contact interaction [1, 2]. Notably, it has been emphasized that the soliton’s center of mass is a collective degree of freedom whose dynamics can show genuine quantum effects. In this vein, Weiss and Castin [3] have calculated the scattering amplitude of a soliton by a potential barrier, which results in a superposition of classically distinct quantum states, namely the soliton being either transmitted or reflected. Similarly, Lewenstein and Malomed [4] have proposed to generate entanglement by the controlled collision of quantum solitons.

A well-known paradigm of genuine quantum dynamics is disorder-induced Anderson localization [5, 6], which has been studied for solitons in different settings some time

ago [7], and also been observed rather recently with ultracold, non-interacting matter waves [8–11] (see also [12]). Motivated by these experimental advances, we have investigated the quantum dynamics of matter-wave solitons in spatially correlated disordered potentials [13]. The first part of the present paper reviews briefly the derivation of an effective Hamiltonian for the center of mass and the resulting localization exponent in an optical speckle potential.

Naturally, there is more to solitons than just their center-of-mass dynamics. Whenever inhomogeneous force fields act on a compound object, the latter responds by adapting its internal configuration as well. For weak forces, the response will be linear and thus described by a (linear) susceptibility. The second part of this paper investigates in more detail how the soliton’s ground-state shape changes under the influence of a weak external potential. We calculate the linear compressibility in general, and then focus on the simple, yet interesting, case of a lattice potential, including a detailed comparison of analytical results to numerical data. This allows us finally to derive quantitative criteria for the external perturbation of the shape to be weak.

## 2 Setting the stage

We describe a weakly interacting Bose–Einstein condensate (BEC) in a quasi-one-dimensional wave guide by its mean-field amplitude  $\phi(z)$ . The Gross–Pitaevskii (GP) free-energy functional, with a given chemical potential  $\mu$  and in a homogeneous wave guide, reads

$$E_0[\phi, \phi^*] = \int dz \left\{ \frac{1}{2} |\partial_z \phi|^2 + \frac{g}{2} |\phi|^4 - \mu |\phi|^2 \right\}. \quad (1)$$

We will use units such that  $\hbar = m = 1$  throughout the following.  $g = 2\omega_{\perp} a$  is the effective interaction constant for

C.A. Müller (✉)

Centre for Quantum Technologies, National University of Singapore, Singapore 117543, Singapore  
e-mail: cord.mueller@nus.edu.sg

a quasi-one-dimensional condensate with s-wave scattering length  $a$  and transverse harmonic trapping frequency  $\omega_{\perp}$ . The cases of repulsive ( $a > 0$ ) and attractive ( $a < 0$ ) interaction correspond to  $g > 0$  and  $g < 0$ , respectively.

Minimizing the free energy  $E_0$  yields the ground state  $\phi_0(z)$ . The chemical potential  $\mu$  thus determines the total number of particles  $N_0 = \int dz n_0(z)$ , with  $n_0(z) = |\phi_0(z)|^2$  being the condensate density. Let us choose periodic boundary conditions, as for a toroidal wave guide with circumference  $L$ . In the case of repulsive interaction  $g > 0$ , both kinetic energy and interaction energy are minimized by spreading the density homogeneously over the entire available length:  $n_0 = \mu/g$  and  $N_0 = L\mu/g$  with  $\mu > 0$ . The corresponding ground-state wave function  $\phi_0 = e^{i\theta_0} \sqrt{\mu/g}$  plays the rôle of a BEC order parameter, featuring an arbitrary global phase  $\theta_0$  that spontaneously breaks the  $U(1)$  gauge invariance of (1). For the ground state of a single Bose–Einstein condensate, we can set  $\theta_0 = 0$ .

An attractive interaction  $g < 0$  rather favors a state where atoms are clustered together. As shown by Kanamoto et al. [14], for large enough system size or chemical potential (i.e. number of particles),  $L|\mu|^{1/2} \gg 1$ , the energetically preferred state is a *soliton*,

$$\phi_0(z - z_0) = \left| \frac{2\mu}{g} \right|^{1/2} \operatorname{sech}[(z - z_0)/\xi] e^{i\theta_0} \tag{2}$$

with a hyperbolic secant envelope, decaying over the length scale  $\xi = |2\mu|^{-1/2}$  known as the condensate healing length. The number of particles is now  $N_0 = 2|2\mu|^{1/2}/|g|$ . Conversely, in a canonical setting with fixed number of particles  $N$ , the chemical potential settles to  $\mu_0 = -1/(2\xi^2) = -g^2 N^2/8 < 0$ .

Note that the solution (2) spontaneously breaks not only the gauge invariance with a phase  $\theta_0$  (that we take to be zero), but also the translational invariance of the energy functional (1). Therefore, the center of mass  $z_0 =: q$  emerges as a dynamical degree of freedom on its own. In the homogeneous situation described by (1), all classical solutions  $q(t) = q_0 + vt$  with constant velocity  $v$  are admissible by Galilean invariance. In a given frame of reference, the classical configuration with minimum kinetic energy is a soliton resting at  $q = q_0$ . Quantum mechanically, however,  $q$  is rather distributed with its ground-state wave function  $\Psi_0(q)$  that obeys the free Schrödinger equation under the given boundary conditions. For periodic boundary conditions, this center-of-mass ground state is the completely delocalized plane wave with momentum  $p_q = 0$ , i.e. the constant  $\Psi_0(q) = L^{-1/2}$ . Contrary to the point of view that the “wave properties of solitons manifest themselves in radiation emitted due to scattering by impurities” [7, p. 53], we take a more general approach along the fundamental principles of quantum mechanics, namely that wave–particle duality is a general feature of all degrees of freedom, to be revealed under appropriate experimental circumstances.

It may seem peculiar to speak of quantum dynamics for the center of mass of a whole collection of atoms, after starting out from a mean-field description for the entire condensate. But it is indeed very common to separate the center of mass from internal variables in interacting systems and moreover exact for two-body forces that only depend on the relative distance between the microscopic constituents. The situation of a soliton, composed of individual atoms held together by attractive contact interactions, is therefore analogous to the situation of, say, an alkali atom composed of a nucleus and electrons held together by the Coulomb force. And, just as one may study the quantum dynamics of entire atoms—not to mention fullerenes or biomolecules [15]—one may indeed equally well study the quantum dynamics of entire solitons as far as their center of mass is concerned.

Consider now the mean-field energy functional in the presence of an external potential  $V(z)$ :

$$E = \int dz \left\{ \frac{1}{2} |\partial_z \phi|^2 + \frac{g}{2} |\phi|^4 + [V(z) - \mu] |\phi|^2 \right\}. \tag{3}$$

We assume that  $V(z)$  is a small perturbation on the energy scale set by  $\mu$ . To lowest order in  $V/|\mu|$ , therefore, the shape of the original soliton will remain unchanged. In contrast, the external potential can never be considered a small perturbation for the center-of-mass dynamics because a finite  $V$  is never small compared to the homogeneous case  $V = 0$ .

At this point, the paper bifurcates. In the following section, we focus on the center of mass. We highlight the quantumness of its dynamics in a disordered potential by discussing the Anderson localization length, as first derived in [13]. As a complement to this work, we will study in Sects. 4 and 5 below how the soliton’s shape is modified by the presence of a weak external potential in the mean-field ground state. Section 6 concludes the paper.

### 3 Anderson localization of a soliton

#### 3.1 Effective Hamiltonian

Assuming a fixed soliton shape, the center of mass  $q$  of  $N$  particles can be described as a collective variable with the ansatz  $\phi(z; q, p_q) = e^{ip_q z/N} \phi_0(z - q)$ . Here, the conjugate momentum  $p_q$  appears in the phase together with a factor  $N^{-1}$  because  $\phi_0$ , (2), is normalized to  $N = 2|2\mu|^{1/2}/|g|$ . Inserting this collective-variable ansatz in the energy functional (3) and integrating over  $z$  yields the effective Hamiltonian

$$H_q = \frac{p_q^2}{2N} + \int dz |\phi_0(z - q)|^2 V(z). \tag{4}$$

This Hamiltonian describes a particle with mass  $N$  evolving in a potential  $\tilde{V}(q) = V * n_0(q)$  that is the convolution of the bare potential with the soliton envelope.

If the bare potential varies only very slowly over one healing length  $\xi = 2/(N|g|)$ , then the soliton feels the sum of forces on its constituents,  $\tilde{V}(q) = NV(q)$ . If on the other hand the potential varies rather rapidly, then the convolution by the soliton density washes out all details on scales smaller than  $\xi$ , and the effective potential is strongly reduced. This is easily illustrated with a lattice potential  $V(z) = V_0 \cos(kz)$ , for which the effective potential is essentially the Fourier transform of the soliton density  $|\phi_0(z - z_0)|^2$  of (2):

$$\tilde{V}(q) = N \frac{\pi k \xi / 2}{\sinh(\pi k \xi / 2)} V_0 \cos(kq). \quad (5)$$

Indeed,  $\tilde{V}(q) \rightarrow NV(q)$  as  $k\xi \rightarrow 0$  and, for  $k\xi \gg 1$ , the amplitude  $V_0 \sim ke^{-\pi k \xi / 2}$  becomes exponentially small.

### 3.2 Correlated disorder

A disordered potential is a random process  $V(z)$  characterized by its moments  $\overline{V(z)}$ ,  $\overline{V(z_1)V(z_2)}$ , etc. Statistically homogeneous disorder is translation invariant after averaging, with  $\overline{V(z)} = \text{const.}$ ,  $\overline{V(z+z_0)V(z_0)} = \overline{V(z)V(0)}$ , etc. Without loss of generality, one can always set  $\overline{V(z)} = 0$  by redefining the zero of energy or shifting  $\mu \mapsto \mu + \overline{V(z)}$  in (3). Thus, the most basic information about the disordered potential is its pair correlator  $\overline{V(z)V(0)} = V_0^2 C(z/\sigma)$ , where  $V_0^2 := \overline{V(z)^2}$  is the variance characterizing the overall strength of disorder. The spatial correlation function  $C(z/\sigma)$  decreases from  $C(0) = 1$  to zero over a characteristic length scale  $\sigma$ , the correlation length of the disorder.

Equivalently, a disordered potential can be seen as a random superposition of plane-wave components  $V_k = L^{-1} \int dz e^{-ikz} V(z)$ . Statistical homogeneity then translates into conservation of total momentum under averaging:  $\overline{V_k V_{k'}} = L^{-1} \delta_{k,-k'} V_0^2 P(k)$ , where the so-called power spectrum  $P(k)$  is the Fourier transform of the real-space correlator  $C(z/\sigma)$ .

For the present case of cold-atom dynamics, we consider in detail optical speckle potentials [16], for which the laws of optics result in a remarkably simple correlation:  $C(z/\sigma) = [\text{sinc}(z/\sigma)]^2$  or

$$P(k) = \pi\sigma \left(1 - \frac{1}{2}|k\sigma|\right) \Theta \left(1 - \frac{1}{2}|k\sigma|\right). \quad (6)$$

The correlation length  $\sigma$  is determined by the wavelength of the laser light and the geometric aperture of the imaging system and can be as short as  $\sigma = 0.26 \mu\text{m}$  [8]. The Heaviside distribution  $\Theta(\cdot)$  in (6) excludes all wave vectors with modulus larger than  $2/\sigma$ , as required by the limit of optical resolution.

The effective potential felt by the soliton's center of mass is the convolution of the bare potential by the soliton density. By virtue of the convolution theorem, the Fourier components of the effective potential are therefore the product

of the bare components times the Fourier components of the density, which already appeared in (5):

$$\tilde{V}_k = N \frac{\pi k \xi / 2}{\sinh(\pi k \xi / 2)} V_k. \quad (7)$$

The statistical properties of the potential affecting the soliton's center of mass are therefore completely determined and readily expressed in Fourier components. For example, the effective power spectrum reads

$$\tilde{P}(k) = N^2 \frac{(\pi k \xi / 2)^2}{\sinh(\pi k \xi / 2)^2} P(k). \quad (8)$$

If the potential is very smooth on the soliton scale  $\xi$ , i.e. has a correlation length  $\sigma \gg \xi$ , the power spectrum  $P(k)$  goes to zero faster than the soliton Fourier envelope, and  $\tilde{P}(k) \approx N^2 P(k)$ . Conversely, if the bare potential is varying very rapidly,  $\sigma \ll \xi$ , the bare spectrum can be approximated in the range  $k\sigma \ll 1$  by its delta-correlation limit  $P(0)$ . Then, the healing length  $\xi$  takes over as the new correlation length with an exponential decay of potential fluctuations as

$$\tilde{P}(k) \approx (N\pi k \xi)^2 P(0) e^{-\pi k \xi}, \quad (9)$$

for  $k\xi \gg 1$ .

### 3.3 Anderson localization exponent

The Hamiltonian of the free soliton,  $p_q^2/2N$ , has the plane-wave eigenfunctions  $\Psi_k(q) \propto e^{ikq}$ . When a small disordered potential is switched on, these extended plane-wave states become exponentially localized. Mathematically rigorous theorems assure that in one dimension, the logarithmically averaged eigenfunctions decay for large distances  $q$  from their origin like [5, 7]

$$\lim_{q \rightarrow \infty} \overline{\log |\Psi(q)|} = -\frac{1}{2} \gamma(k) q. \quad (10)$$

The corresponding localization exponent, or inverse localization length,  $\gamma(k)$ , can be calculated perturbatively (for generic values of  $k$ , i.e. away from the band center  $k = 0$  or other singular points) in powers of the strength of the disordered potential. To second order in  $V_0$ , in the so-called Born approximation, the localization exponent reads  $\gamma(k) = (k^2 V_0^2 / 4E_k^2) P(2k)$ , with  $E_k = \hbar^2 k^2 / 2m$  the free kinetic energy [17–19]. The potential correlator is evaluated at momentum  $2k$ , since it is the elementary backscattering process  $k \rightarrow -k$  that is eventually responsible for Anderson localization in one dimension.

For the soliton, we have  $\tilde{E}_k = k^2 / (2N)$  and scattering by the effective potential  $\tilde{V}_k$ , such that the localization exponent is predicted to be

$$\tilde{\gamma}(k) = \frac{N^2 V_0^2}{k^2} \tilde{P}(2k) = \frac{N^4 V_0^2}{k^2} \frac{(\pi k \xi)^2}{\sinh(\pi k \xi)^2} P(2k). \quad (11)$$

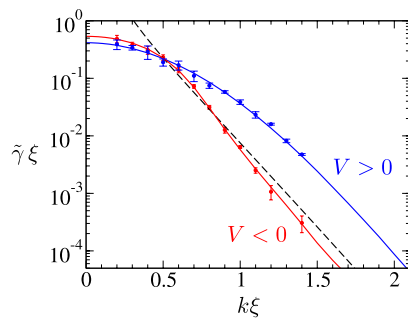


**Fig. 1** Log-linear plot of the soliton localization exponent  $\tilde{\gamma}(k)$  versus its center-of-mass wave vector  $k$ , in units of the soliton width  $\xi$ . Circles are numerical results obtained by diagonalizing the Hamiltonian (4) and solid lines are the result of a transfer-matrix calculation [13, 20], for red- and blue-detuned speckle potentials with  $V_0 = \pm 8 \times 10^{-5} |\mu|$ , respectively, and a correlation length  $\sigma = 0.28\xi \approx 0.26 \mu\text{m}$ . The Born approximation, (11), is shown as a dashed line. The overall exponential decrease for  $k\xi \gg 1$  and  $k\sigma \ll 1$  is clearly visible

Figure 1 shows this prediction, together with numerical data, obtained by both exact diagonalization of the Hamiltonian (4) and a transfer-matrix approach, respectively [13, 20]. We have chosen realistic experimental parameters:  $N = 100$   $^7\text{Li}$  atoms with scattering length  $a = -3 \text{ nm}$  in a transverse trap with  $\omega_{\perp} = 2\pi \times 5 \text{ kHz}$  form a soliton of size  $\xi \approx 100 \mu\text{m}/N \approx 1 \mu\text{m}$ . We consider an optical speckle potential with amplitude  $V_0 = \pm 8 \times 10^{-5} |\mu|$ , i.e. both the red-detuned case with  $V_0 < 0$  and the blue-detuned case with  $V_0 > 0$ . Since the speckle potential has a non-Gaussian, skewed distribution, the full localization exponent depends on the absolute sign of  $V_0$ , an effect that the lowest-order Born approximation  $O(V_0^2)$  cannot capture. However, the overall exponential decrease for  $k\xi \gg 1$  is correctly predicted.

These results show that the localization length,  $\tilde{\gamma}^{-1}$ , of not-too-fast solitons with  $k\xi \approx 1$  is in the sub-mm range that is measurable in current experiments on localization of non-interacting matter waves [8]. Further results can be found in [13], such as the expected density distribution of the final soliton position, depending on initial trapping conditions.

But what about the emission of radiation due to scattering by impurities, as discussed at length by Gredeskul and Kivshar [7] and others? It is important to realize that we specifically focus on smooth, spatially correlated potentials that are expected to provoke considerably less excitation than isolated,  $\delta$ -like impurities. Nonetheless, it is clearly important to know the precise effects of the external disorder on the soliton shape. Some light on this issue will be shed in the following sections.

#### 4 Linear response for the mean-field ground state

The previous results on the disorder-induced localization of a soliton have been derived with the effective Hamil-

tonian (4) as the only ingredient. There, the soliton shape was assumed to be completely unaffected by the external potential. Although  $|V| \ll |\mu|$  is probably a sufficient condition for this to be valid [20], as such it cannot be a satisfying, namely necessary, criterion. Indeed, a potential with a large amplitude  $V \gg |\mu|$  but fluctuating only on very long length scales hardly deforms the soliton if its variation over the soliton size,  $\xi dV/dz$ , is very small. Conversely, the amplitude of an interacting condensate cannot follow very rapid potential oscillations with a wavelength much smaller than  $\xi$ , since this would cost too much kinetic energy in (12). In this case, only strongly smoothed fluctuations are expected to appear, just as in the repulsive case [21]. In order to sharpen the picture, we therefore set out to compute the mean-field soliton deformation as a function of the potential's amplitude and wave vector.

A small deformation of the ground state can be described by an expansion over a complete set of elementary excitations, such as described by Bogoliubov theory. In general, the Bogoliubov theory of condensate excitations in inhomogeneous potentials can be formulated as a saddle-point expansion of the mean-field energy functional [22–24] and comprises two important steps: in a first step, the deformed ground state is determined as a functional of the external potential. In a second step, the quadratic excitations around this deformed ground state are determined. In order to arrive at meaningful results with all effects to a given order of  $V$  taken properly into account, the first step is a vital prerequisite for carrying out the second. In the present contribution, we shall content ourselves with taking step 1, the consistent calculation of the mean-field ground-state deformation caused by a weak, but otherwise arbitrary, external potential  $V(z)$ .

For the repulsive case with its homogeneous ground-state density  $n_0 = \mu/g$ , such a linear response to an external inhomogeneous potential can be computed rather easily, taking advantage of Fourier decomposition; for applications to disordered potentials, see e.g. the work of Giorgini et al. [25] and Sanchez-Palencia [21]. For a soliton with its inhomogeneous ground-state density, a very similar linear response scheme, technically slightly more demanding but perhaps also more interesting, is presented in the following.

##### 4.1 Density response

Taking our cue from Giorgini et al., we start with the GP functional (1) in density-phase representation  $\phi(z) = \sqrt{n(z)}e^{i\theta(z)}$ :

$$E_0 = \int dz \left\{ \frac{1}{2} [(\partial_z \sqrt{n})^2 + n(\partial_z \theta)^2] + \frac{g}{2} n^2 - \mu n \right\}. \quad (12)$$

Since the perturbation  $\int dV(z)n(z)$  couples to the density, the deformed ground-state density reads  $n(z) = n_0(z) +$

$\delta n(z)$ , where the shift within linear response is given by

$$\delta n(z) = - \int dz' \chi(z, z') V(z') + O(V^2). \tag{13}$$

The density–density susceptibility (essentially the compressibility) is defined via its functional inverse,

$$\chi^{-1}(z, z') = \frac{\delta^2 E_0}{\delta n(z) \delta n(z')} \Big|_0 \tag{14}$$

$$= \frac{1}{2} \left[ \frac{1}{2n_0(z)} \partial_z \partial_{z'} - \frac{\mu}{n_0(z)} + 3g \right] \delta(z - z'). \tag{15}$$

Unlike in the repulsive case with  $n_0$  constant where the inverse is easily computed in Fourier modes [25], here we have an inhomogeneous density  $n_0(z)$  and thus  $\chi^{-1}$  is difficult to invert. We bypass this difficulty with a second approach in the upcoming section and come back to the compressibility in Sect. 4.3 below.

### 4.2 Wave-function response

The mean-field ground-state wave function  $\phi(z)$ , which can be taken real, satisfies  $\delta E / \delta \phi^* = 0$ , known as the stationary GP equation

$$\left[ -\frac{1}{2} \partial_z^2 + g\phi(z)^2 - \mu + V(z) \right] \phi(z) = 0. \tag{16}$$

Following Sanchez-Palencia [21], we develop  $\phi(z) = \phi_0(z - z_0) + \delta\phi(z - z_0)$  around the ground-state solution (2) by treating  $\delta\phi$  as a small quantity of order  $V/|\mu|$ . Linearizing gives

$$\left[ -\frac{1}{2} \partial_z^2 + 3gn_0(z - z_0) - \mu \right] \delta\phi(z - z_0) = -V(z)\phi_0(z - z_0). \tag{17}$$

Measuring distances in units of  $\xi$  around  $z_0$ , i.e. writing  $z - z_0 = \xi x$  and dividing by  $2|\mu| = \xi^{-2}$ , one finds the linear equation

$$\left[ -\frac{1}{2} \partial_x^2 - 3 \operatorname{sech}(x)^2 + \frac{1}{2} \right] \delta\varphi(x) = -\frac{V(z_0 + \xi x)}{2|\mu|} \varphi_0(x) \tag{18}$$

for the dimensionless shift  $\delta\varphi(x) = \sqrt{\xi} \delta\phi(\xi x)$ . This equation is of the form

$$\left[ H_0 + \frac{1}{2} \right] \delta\varphi(x) = W(x) \tag{19}$$

with  $H_0 = p^2/2 - 3 \operatorname{sech}(x)^2$  the Hamiltonian of the  $\operatorname{sech}^2$ -potential well, the well-known Pöschl–Teller potential [26].

On the right-hand side, one has an external source term

$$W(x) = -\varphi_0(x) \frac{V(z_0 + \xi x)}{2|\mu|}. \tag{20}$$

Computing  $\delta\varphi$  then only requires us to invert  $H_0$ . Fortunately for us, this is very simple to do because all potentials of the form  $-\frac{1}{2}v(v + 1) \operatorname{sech}(x)^2$  with integer  $v$  are supersymmetric partners of the free-particle case  $v = 0$ , and their eigenstates and eigenenergies are perfectly known; for a brief and pedagogical introduction to these issues, see [27]. The case  $v = 2$  of interest here is treated in detail by Lekner [28].  $H_0$  admits two bound states,

$$\psi_0(x) = \frac{\sqrt{3}}{2} \operatorname{sech}(x)^2, \tag{21}$$

$$\psi_1(x) = \sqrt{\frac{3}{2}} \operatorname{sech} x \tanh x \tag{22}$$

with eigenenergies  $E_0 = -2$  and  $E_1 = -\frac{1}{2}$  (in units of  $2|\mu|$ ), respectively, as well as scattering eigenstates

$$\psi_k(x) = \frac{e^{ikx}}{[2\pi]^{1/2}} \frac{k^2 - 2 + 3 \operatorname{sech}(x)^2 + 3ik \tanh x}{[(1 + k^2)(4 + k^2)]^{1/2}} \tag{23}$$

with free kinetic eigenenergy  $E_k = k^2/2$ ,  $k \in \mathbb{R}$ . These eigenmodes have appeared repeatedly in one form or another in the soliton literature (cf. a recent paper by Castin [29] and works cited therein), but often without reference to the underlying supersymmetry of the Pöschl–Teller potential.

We can expand the deformation  $\delta\varphi$  over this orthonormal basis set of eigenfunctions,

$$\delta\varphi(x) = \alpha_0 \psi_0(x) + \alpha_1 \psi_1(x) + \int dk \alpha_k \psi_k(x), \tag{24}$$

and then determine the coefficients by projecting (18) onto each eigenfunction:

$$\left( E_j + \frac{1}{2} \right) \alpha_j = \int dy \psi_j^*(y) W(y). \tag{25}$$

Interestingly, the coefficient  $\alpha_1$  of the first excited bound state  $j = 1$  remains undetermined because  $E_1 = -1/2$  of  $H_0$  is exactly compensated by the  $+1/2$ . In other words, this mode appears as a zero-energy eigenmode of the linear response kernel [13, 20].<sup>1</sup> This has a simple, yet profound, physical explanation: because  $\psi_1(x) = -\sqrt{3/N} \partial_x \varphi_0(x)$ , the deformation  $\varphi_0(x) + \alpha_1 \psi_1(x) = \varphi_0(x + \delta x) + O(V^2)$  simply shifts the center of mass by  $\delta x = -\alpha_1 \sqrt{3/N}$ . Thus, we find, as argued in Sect. 1 above, that the soliton’s center

<sup>1</sup>Similarly, the phase mode associated with the spontaneously broken  $U(1)$  symmetry is a zero-energy mode of Bogoliubov theory; see [30, 31].

of mass is an independent dynamical variable that is influenced non-perturbatively by the external potential.

Let us then assume in the following that the soliton’s center of mass has reached a position such that the external potential does not accelerate it any more, namely that the right-hand side of (25) for  $j = 1$  vanishes. A sufficient condition for this is that the external potential  $V(z)$  is (locally) an even function around the soliton position  $z_0$ . Then, the soliton shape deformation reads

$$\delta\varphi(x) = \alpha_0\psi_0(x) + \int dk \alpha_k \psi_k(x) \tag{26}$$

with (25) determining the coefficients  $\alpha_0$  and  $\alpha_k$  as linear functions of the external potential  $V(z)$ , scaling by construction as  $V/|\mu|$ . In Sect. 5 below, we will study the scaling with the wave vector for a simple lattice potential.

### 4.3 Real-space response kernel

By linearity, the soliton shape deformation (26) can also be conveniently expressed as a functional of the potential (20),

$$\delta\varphi(x) = \int dy K(x, y)W(y), \tag{27}$$

with a symmetric kernel given by

$$K(x, y) = -\frac{2}{3}\psi_0(x)\psi_0(y) + 2 \int dk \frac{\psi_k(x)\psi_k^*(y)}{1+k^2}. \tag{28}$$

The  $k$ -integral can be evaluated, leading after some algebra to the following closed-form expression for the real-space response kernel:

$$K(x, y) = \frac{1}{4} \operatorname{sech} x \tanh x \operatorname{sech} y \tanh y \times [\cosh 2x + \cosh 2y - |\sinh 2x - \sinh 2y| - 4 \operatorname{csch} x \operatorname{csch} y \sinh |x - y| - 6|x - y|]. \tag{29}$$

Equations (27) and (29) together with (20) provide a prêt-à-calculer expression of the soliton shape as a function of any given potential  $V(z)$ . While soliton deformation in external potentials is certainly not a new topic and has been considered in a rather large number of different contexts (see e.g. [7] and references therein), to our knowledge this useful expression of the linear-response kernel is new.

This solution determines also the compressibility introduced in Sect. 4.1. From  $n(z) = [\phi_0(z - z_0) + \delta\phi(z)]^2 = n_0(z - z_0) + \delta n(z) + O(V^2)$ , it follows that  $\delta n(z) = 2\phi_0(z - z_0)\delta\phi(z)$ , and we can read off from the previous expressions that the density–density susceptibility of (13) is given by

$$\chi(z, z') = 2\xi\phi_0(z - z_0)K\left(\frac{z - z_0}{\xi}, \frac{z' - z_0}{\xi}\right)\phi_0(z' - z_0). \tag{30}$$

The compressibility  $\chi(z, z')$  does not depend solely on  $z - z'$ , as it would in homogeneous systems. Instead, it refers to a distinguished point, namely the soliton position  $z_0$ , and is only invariant under simultaneous translation of all three coordinates  $z, z', z_0$ .

### 4.4 Grand-canonical versus canonical deformation

The previous derivation used the grand-canonical setting at fixed chemical potential  $\mu$ . The corresponding soliton deformation  $\delta\varphi(x) =: \delta\varphi(x)|_\mu$  and density shift  $\delta n(z) =: \delta n(z)|_\mu$  do not conserve the total number of particles. The change in particle number to order  $V/|\mu|$  reads  $\delta N = \int dz \delta n(z) = - \int \int dz dz' \chi(z, z')V(z')$ .

In order to calculate the soliton deformation at fixed number of particles  $N$ , i.e. to compensate  $\delta N$ , the chemical potential has to be adjusted. Since  $|\mu| = g^2 N^2/8$ , the required shift is  $\delta|\mu| = -2|\mu|\delta N/N$ . Inserting (30) and performing the integral over  $z$  yields the relatively simple expression

$$\frac{\delta|\mu|}{2|\mu|} = - \int dy (1 - y \tanh y) \operatorname{sech}(y)^2 \frac{V(z_0 + \xi y)}{2|\mu|}. \tag{31}$$

Since the grand-canonical deformation  $\delta\varphi|_\mu$  given by (27) is already of order  $V/|\mu|$ , it is not affected by this shift to lowest order, but the original soliton background is changed:  $\varphi_0(x)|_N = \varphi_0(x)|_\mu + \partial_{|\mu|}\varphi_0(x)\delta|\mu|$ . Altogether, we find for the canonical soliton deformation at fixed number of particles  $N$

$$\delta\varphi(x)|_N = \delta\varphi(x)|_\mu + \frac{\delta|\mu|}{2|\mu|}(1 - x \tanh x)\varphi_0(x), \tag{32}$$

where  $\delta\varphi(x)|_\mu$  is given by (27), and  $\delta|\mu|/2|\mu|$  by (31), with  $\mu = -g^2 N^2/8$ ,  $\xi = 2/(N|g|)$  and  $\varphi_0(x) = \sqrt{N/2} \times \operatorname{sech} x$  in all expressions. This formula, together with the kernel (29), constitutes the main achievement of this work.

## 5 Special case: lattice potential

In order to illustrate the above results, we study in detail the case of a simple lattice potential with reduced wave vector  $k_0 = k\xi$ :

$$V(\xi x) = -V_0 \cos(k_0 x) \tag{33}$$

with  $V_0 \geq 0$  such that the center of mass of a soliton prepared at  $z_0 = 0$  (modulo the lattice period) sits in a potential minimum, where it remains classically. The limit  $k_0 \ll 1$  reduces to the particular case of a purely harmonic confinement studied recently by Castin [29]. Since the soliton deformation  $\delta\varphi$  is a linear functional of  $V$ , more general potentials (such as disordered ones) can be studied by applying the following results to their Fourier components.

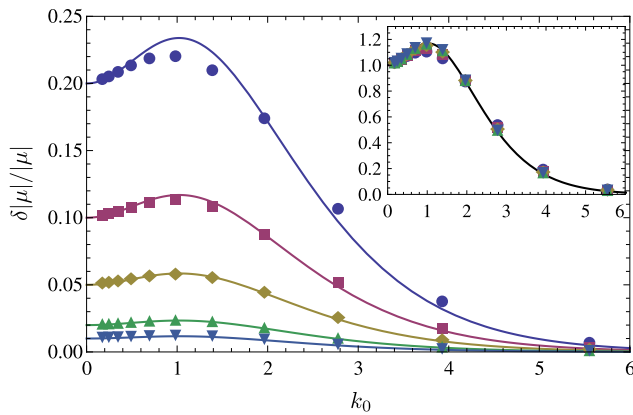


**Fig. 2** Relative shift in the chemical potential,  $\delta|\mu|/|\mu|$ , as a function of  $k_0$  in a lattice of various depths  $V_0/|\mu| \in \{0.2, 0.1, 0.05, 0.02, 0.01\}$  (top to bottom). Symbols: numerical results from an imaginary-time integration of the GP equation. Solid lines: linear-response prediction, (34). The inset shows the collapsed data, i.e. the raw data divided by  $V_0/|\mu|$ . As  $k_0 \gg 1$  or  $V_0/|\mu| \ll 1$ , the shift is correctly predicted and, as expected, small

### 5.1 Chemical potential shift

First of all, the chemical potential shift (31) evaluates to

$$\frac{\delta|\mu|}{|\mu|} = \frac{V_0}{|\mu|} \frac{(\pi k_0/2)^2}{\sinh(\pi k_0/2)^2} \cosh \frac{\pi k_0}{2}. \quad (34)$$

As  $k_0 = k\xi \rightarrow 0$ , one finds  $\delta|\mu| = V_0$  as expected, since this exactly compensates a global potential offset  $-V_0$ . Also, not surprisingly, the shift vanishes as  $k_0 \rightarrow \infty$  at fixed  $V_0$ , since the condensate cannot follow these rapid variations. But, it may perhaps come as a surprise that the behavior as a function of  $k_0$  described by (34) is non-monotonic.

We can compare these predictions to the results of a numerical integration of the imaginary-time GP equation  $\partial_\tau \varphi(x, \tau) = -H\varphi(x, \tau)$  that describes a steepest-descent trajectory towards the minimum of the canonical energy functional (i.e. (12) with  $\mu = 0$ ) [32]. This dynamics is not unitary, and the correct normalization to  $N$  must be re-established at each time step. When the stationary state is reached,  $\varphi(x, \tau) = e^{-\mu\tau}\varphi(x)$ , the chemical potential is easily extracted from the required global renormalization factor. Figure 2 shows the measured relative shift  $\delta|\mu|/|\mu|$  as a function of  $k_0$  for various potential strengths ( $N = 100$ ). The analytical prediction (34) is indeed found to be correct for  $V_0 \ll |\mu|$ . The inset shows the collapsed data obtained after division by  $V_0/|\mu|$ , clearly featuring the interesting  $k_0$ -dependence, with the maximal shift reached close to  $k_0 = 1$ .

### 5.2 Expansion coefficients and small parameter

The expansion coefficients (25) read

$$\alpha_0 = -\frac{V_0}{2|\mu|} \sqrt{\frac{N}{6}} \frac{\pi}{2} (1+k_0^2) \operatorname{sech} \frac{\pi k_0}{2}, \quad (35)$$

$$\alpha_k = -\frac{V_0}{2|\mu|} \frac{\sqrt{\pi N}}{4} \frac{1+k^2-3k_0^2}{(1+k^2)^{3/2}(4+k^2)^{1/2}} \times \left[ \operatorname{sech} \frac{\pi}{2}(k+k_0) + \operatorname{sech} \frac{\pi}{2}(k-k_0) \right]. \quad (36)$$

All coefficients scale as  $V_0/|\mu|$  by construction. As a function of  $k_0$ , the bound-state coefficient  $\alpha_0 \sim k_0^2 e^{-\pi k_0/2}$  becomes exponentially small for a rapidly fluctuating potential  $k_0 \gg 1$  (cf. the qualitatively similar behavior of the effective potential (5)) and thus does not contribute substantially in this limit. Away from  $|k| = k_0 \gg 1$ , the coefficients  $\alpha_k$  are also exponentially small. However, the resonant amplitudes  $\alpha_{\pm k_0} \sim k_0^{-2}$  are only algebraically small. We therefore conclude that the modes  $\pm k_0$  contribute dominantly, imprinting a pure sinusoidal wave onto the soliton, with an overall weight scaling as

$$\frac{V_0}{|\mu|k_0^2} = \frac{2V_0}{k^2} = \frac{V_0}{E_k}. \quad (37)$$

In this smoothing regime, completely analogous to the repulsive case [21], the healing length (or chemical potential) drops out, and the small parameter of the expansion rather is the ratio of the potential amplitude to the kinetic energy  $E_k$  associated with the spatial lattice wave vector  $k$ .

### 5.3 Real-space response

Unfortunately, even for the simple lattice potential (33), the integral (27) over the kernel (29) cannot be evaluated in simple closed form. However, it is easily calculated numerically. Figure 3 shows how the unperturbed soliton ground state  $\varphi_0(x) = \sqrt{N/2} \operatorname{sech} x$  with  $N = 100$  particles is deformed by a lattice potential with a rather large amplitude,  $V_0 = 0.2|\mu|$ , and intermediate lattice wave vector,  $k_0 = 5\pi/8 \approx 1.9635$ . The prediction from the linear-response theory matches the full result quite well, considering that the perturbation is rather strong. To reach this agreement, it is essential to take into account the chemical potential shift according to (32). The deviations  $\delta\varphi(x)$  are also shown in dashed lines. One clearly observes a concentration of density around the potential minimum, as well as density depressions around the first potential maxima.

To check the validity and precision of the linear response, we plot the deformation in direct comparison to the data from the numerical solution, together with the potential in Fig. 4 for fixed intermediate wave vector  $k_0 = 5\pi/8$  and various potential strengths  $V_0/|\mu| \in \{1, 0.2, 0.05, 0.01\}$ . By parity, we can restrict the plots to  $x \geq 0$ . As expected, the linear response approaches the full solution very well as soon as  $V_0 \ll |\mu|$ .

Finally, Fig. 5 shows the same data for fixed potential strength  $V_0 = 0.1|\mu|$  and various wave vectors  $k_0 \in 5\pi\{\frac{1}{16}, \frac{1}{8}, \frac{1}{4}, \frac{1}{2}\}$ . Note that the vertical axis retains the same

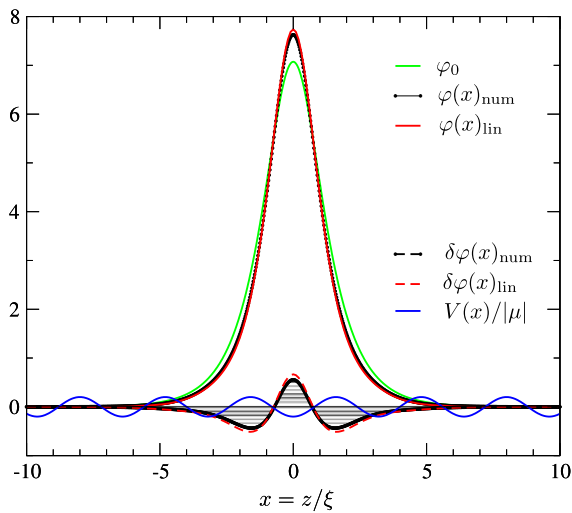


**Fig. 3** A soliton amplitude (green:  $\varphi_0(x)$ ) containing  $N = 100$  particles and centered at  $x = 0$  is deformed by the lattice potential (33) with  $V_0 = 0.2|\mu|$  and wave vector  $k_0 = 5\pi/8$  (blue:  $V(x)/|\mu|$ ). The numerically calculated GP ground state (black:  $\varphi(x)_{\text{num}}$ ) is very well approximated by the linear response result (red:  $\varphi(x)_{\text{lin}}$ ) given by (32). The respective deviations  $\delta\varphi(x)$  are also shown in dashed lines: the amplitude enhancement around the potential minimum at  $x = 0$  is clearly visible, just as the amplitude depression around the first potential maxima

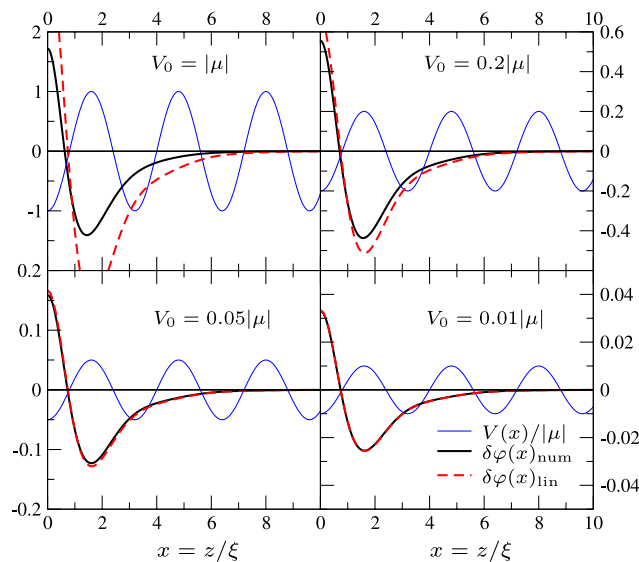


**Fig. 4** Deformation of the soliton shape by a lattice potential (blue:  $V(x)/|\mu|$ ) of fixed wave vector  $k_0 = 5\pi/8$  and various amplitudes  $V_0$ . The linear-response result, (32) (dashed red:  $\delta\varphi(x)_{\text{lin}}$ ), approaches the numerically obtained ground-state deformation (solid black:  $\delta\varphi(x)_{\text{num}}$ ) as  $V_0/|\mu| \rightarrow 0$

scaling in all four plots. As expected from the discussion in Sect. 5.2 above, the linear response becomes increasingly accurate for larger  $k$  vectors, as the deformation itself becomes very small. The last set of data shows an almost pure sinusoidal deformation. Indeed, in the limit  $k_0 \gg 1$ , one can extract the leading contribution of (27) by partial integration

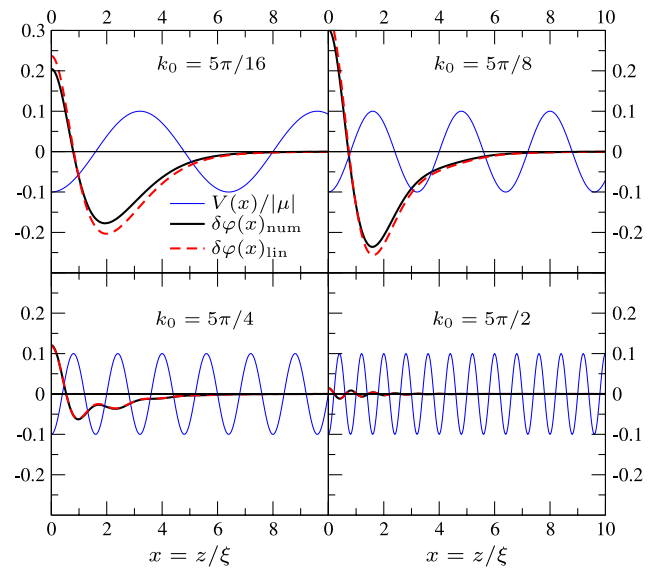


**Fig. 5** Deformation of the soliton shape by a lattice potential (blue:  $V(x)/|\mu|$ ) of fixed amplitude  $V_0 = 0.1|\mu|$  and various wave vectors  $k_0$ . The linear-response result, (32) (dashed red:  $\delta\varphi(x)_{\text{lin}}$ ), approaches the numerically obtained ground-state deformation (black:  $\delta\varphi(x)_{\text{num}}$ ) as  $k_0 \gg 1$

and finds

$$\delta\varphi(x) = \frac{V_0}{E_k} \varphi_0(x) \cos k_0 x \tag{38}$$

up to higher orders in  $V_0/E_k = 2V_0/k^2$ .

### 6 Concluding remarks

In this article, we elaborated on two important aspects of bright cold-atom solitons in inhomogeneous external potentials. Firstly, we discussed the quantum dynamics of the soliton’s center of mass in a disordered, spatially correlated potential. The center-of-mass wave function is predicted to show Anderson localization with a localization length that can be estimated using the Born approximation of perturbation theory and is shown to be in an experimentally relevant range.

Secondly, we calculated the imprint of a weak external potential on the soliton mean-field shape in the ground state. For this, we determined the linear-response kernel, for both the wave function and the local density, as well as the chemical potential shift. Amusingly, this can be done rather easily using the supersymmetric quantum mechanics of the Pöschl–Teller or  $\text{sech}^2$ -potential well. Finally, a detailed comparison to the numerically calculated ground-state solution is presented for a pure lattice potential with amplitude  $V_0$  and wave vector  $k$ . The small parameter of the linear response is  $V_0/|\mu|$  in the regime  $k\xi \approx 1$  of a potential varying on the scale of the soliton width. In the limit  $k\xi \rightarrow 0$ ,

one recovers the case of harmonic confinement, studied recently by Castin [29]. Here, the small parameter for the soliton deformation (27) is  $V_0 k^2 \xi^2 / 2|\mu| = (\omega_0/2|\mu|)^2$  in terms of the harmonic trapping frequency  $\omega_0$ . In the smoothing limit  $k\xi \gg 1$  of a rapidly fluctuating potential, the condensate amplitude shows a pure sinusoidal imprint, the small parameter being  $V_0/E_k$ .

Until now, we have discussed the center-of-mass quantum dynamics for fixed shape on the one hand, and the static properties of the mean-field ground-state shape on the other. From the latter, we have learned that the impact on the soliton shape is indeed small for small  $V_0/|\mu|$ . In other words, the external potential cannot easily excite the internal modes since these have a gapped spectrum. Therefore, whenever the soliton moves slowly within a smooth potential, it is slightly polarized, but only adiabatically and reversibly (just as, say, an alkali atom is polarized in an optical dipole potential). Therefore, we can expect the center-of-mass quantum dynamics to be unharmed by shape excitations as long as the gap  $|\mu|$  remains large compared to all other energies.

It must be kept in mind, however, that Anderson localization is an interference effect relying on perfect phase coherence, at least over the time and distance needed to observe it. Already, very small decoherence can kill this effect. For cold-atom solitons, the most dangerous sources of decoherence arguably are scattering of background-gas atoms (cf. the analogous case of fullerenes [33]) and three-body collisions, both of which can in principle be minimized in the experiment. However, if the movement of a soliton inside a disordered potential were to radiate permanent excitations, as discussed for the case of isolated point impurities in [7], then this would constitute an intrinsic source of decoherence. The detailed study of such effects, well beyond the simple mean-field estimate for the ground state presented here, is left for future research.

**Acknowledgements** This work is supported by the National Research Foundation & Ministry of Education, Singapore. It was initiated in fiery discussions with K. Sacha, J. Zakrzewski and D. Delande at Laboratoire Kastler Brossel (Paris) while the author held a research fellowship from Mairie de Paris. Helpful input by B. Grémaud is gratefully acknowledged.

## References

1. L. Khaykovich, F. Schreck, G. Ferrari, T. Bourdel, J. Cubizolles, L.D. Carr, Y. Castin, C. Salomon, *Science* **296**, 1290 (2002)
2. K.E. Strecker, G.B. Partridge, A.G. Truscott, R.G. Hulet, *Nature* **417**, 150 (2002)
3. C. Weiss, Y. Castin, *Phys. Rev. Lett.* **102**, 010403 (2009)
4. M. Lewenstein, B.A. Malomed, *New J. Phys.* **11**, 113014 (2009)
5. I.M. Lifshitz, S.A. Gredeskul, L.A. Pastur, *Introduction to the Theory of Disordered Systems* (Wiley, New York, 1988)
6. C.A. Müller, D. Delande, [arXiv:1005.0915](https://arxiv.org/abs/1005.0915) (2010)
7. S.A. Gredeskul, Y.S. Kivshar, *Phys. Rep.* **216**, 1 (1992)
8. J. Billy, V. Josse, Z. Zuo, A. Bernard, B. Hambrecht, P. Lugan, D. Clement, L. Sanchez-Palencia, P. Bouyer, A. Aspect, *Nature* **453**, 891 (2008)
9. G. Roati, C. D'Errico, L. Fallani, M. Fattori, C. Fort, M. Zaccanti, G. Modugno, M. Modugno, M. Inguscio, *Nature* **453**, 895 (2008)
10. L. Sanchez-Palencia, M. Lewenstein, *Nat. Phys.* **6**, 87 (2010)
11. G. Modugno, *Rep. Prog. Phys.* **73**, 102401 (2010)
12. M. Albert, P. Leboeuf, *Phys. Rev. A* **81**, 013614 (2010)
13. K. Sacha, C.A. Müller, D. Delande, J. Zakrzewski, *Phys. Rev. Lett.* **103**, 210402 (2009)
14. R. Kanamoto, H. Saito, M. Ueda, *Phys. Rev. A* **67**, 013608 (2003)
15. L. Hackermüller, S. Uttenthaler, K. Hornberger, E. Reiger, B. Brezger, A. Zeilinger, M. Arndt, *Phys. Rev. Lett.* **91**, 090408 (2003)
16. D. Clément, A.F. Varón, J.A. Retter, L. Sanchez-Palencia, A. Aspect, P. Bouyer, *New J. Phys.* **8**, 165 (2006)
17. L. Sanchez-Palencia, D. Clement, P. Lugan, P. Bouyer, G.V. Shlyapnikov, *A. Aspect, Phys. Rev. Lett.* **98**, 210401 (2007)
18. P. Lugan, A. Aspect, L. Sanchez-Palencia, D. Delande, B. Grémaud, C.A. Müller, C. Miniatura, *Phys. Rev. A* **80**, 023605 (2009)
19. E. Gurevich, O. Kenneth, *Phys. Rev. A* **79**, 063617 (2009)
20. K. Sacha, D. Delande, J. Zakrzewski, *Acta Phys. Pol. A* **116**, 772 (2009)
21. L. Sanchez-Palencia, *Phys. Rev. A* **74**, 053625 (2006)
22. C. Gaul, C.A. Müller, *Europhys. Lett.* **83**, 10006 (2008)
23. C. Gaul, C.A. Müller, [arXiv:1009.5448](https://arxiv.org/abs/1009.5448) (2010)
24. C. Gaul, C.A. Müller, [arXiv:1101.4781](https://arxiv.org/abs/1101.4781) (2011)
25. S. Giorgini, L. Pitaevskii, S. Stringari, *Phys. Rev. B* **49**, 12938 (1994)
26. G. Pöschl, E. Teller, *Z. Phys.* **83**, 143 (1933)
27. L.J. Boya, *Eur. J. Phys.* **9**, 139 (1988)
28. J. Lekner, *Am. J. Phys.* **75**, 1151 (2007)
29. Y. Castin, *Eur. Phys. J. B* **68**, 317 (2009)
30. M. Lewenstein, L. You, *Phys. Rev. Lett.* **77**, 3489 (1996)
31. Y. Castin, R. Dum, *Phys. Rev. A* **57**, 3008 (1998)
32. F. Dalfovo, S. Stringari, *Phys. Rev. A* **53**, 2477 (1996)
33. K. Hornberger, S. Uttenthaler, B. Brezger, L. Hackermüller, M. Arndt, A. Zeilinger, *Phys. Rev. Lett.* **90**, 160401 (2003)